THE JOURNAL OF BIOLOGICAL CHEMISTRY VOL. 284, NO. 42, pp. 29125–29135, October 16, 2009

Ovol2 Suppresses Cell Cycling and Terminal Differentiation of Keratinocytes by Directly Repressing c-*Myc* and *Notch1*[*][S]

Received for publication, April 15, 2009, and in revised form, August 8, 2009 Published, JBC Papers in Press, August 21, 2009, DOI 10.1074/jbc.M109.008847

Julie Wells[‡], Briana Lee[‡], Anna Qianyao Cai[§], Adrine Karapetyan[¶], Wan-Ju Lee[‡], Elizabeth Rugg[¶], Satrajit Sinha[‖], Qing Nie[§], and Xing Dai[‡1]

From the [‡]Department of Biological Chemistry, School of Medicine, the [§]Department of Mathematics and Center for Mathematical and Computational Biology, and the [¶]Department of Dermatology, University of California, Irvine, California 92697 and the [‖]Department of Biochemistry, The State University of New York, Buffalo, New York 14203

Ovol2 belongs to the Ovo family of evolutionarily conserved zinc finger transcription factors that act downstream of key developmental signaling pathways including Wg/Wnt and BMP/TGF-β. We previously reported Ovol2 expression in the basal layer of epidermis, where epidermal stem/progenitor cells reside. In this work, we use HaCaT human keratinocytes to investigate the cellular and molecular functions of Ovol2. We show that depletion of Ovol2 leads to transient cell expansion but a loss of cells with long term proliferation potential. Mathematical modeling and experimental findings suggest that both faster cycling and precocious withdrawal from the cell cycle underlie this phenotype. Ovol2 depletion also accelerates extracellular signal-induced terminal differentiation in two- and three-dimensional culture models. By chromatin immunoprecipitation, luciferase reporter, and functional rescue assays, we demonstrate that Ovol2 directly represses two critical downstream targets, c-*Myc* and *Notch1*, thereby suppressing keratinocyte transient proliferation and terminal differentiation, respectively. These findings shed light on how an epidermal cell maintains a proliferation-competent and differentiation-resistant state.

The *Ovo* gene family encodes evolutionarily conserved proteins including members from *Caenorhabditis elegans*, *Drosophila*, *Zebrafish*, chick, and mammals. Ovo proteins contain four DNA-binding C_2H_2 zinc fingers at the C termini and possess transcriptional regulatory activities (1–5). *Drosophila ovo*, the founding member of the family, acts genetically downstream of Wg (fly Wnt homolog) and DER (fly epidermal growth factor receptor homolog) signaling pathways and is required for epidermal denticle formation and oogenesis (6–8). We and others have identified mammalian *Ovol* (*Ovo-like*) genes, including *Ovol1* (*movo1*), *Ovol2* (*movo2*), and *Ovol3* (*movo3*) in mice and *OVOL1*, *OVOL2*, and *OVOL3* in humans (9–12). Mammalian *Ovol/OVOL* (referred to as *Ovol* from here on) genes also appear to reside downstream of key developmental signaling pathways. For instance, *Ovol1* is activated by the β-catenin-LEF1 complex, downstream effectors of Wnt signaling (13), and is a downstream target of TGF-β/BMP7-Smad4 signaling (14, 15). A functional *Ovol1* gene is required for multiple developmental processes, including that of epidermis, hair follicles, kidney, and male germ cell differentiation (2, 4, 10). In both epidermis and testis, Ovol1 restricts the boundary of late progenitor cells during development by promoting cell cycle exit (2, 4). Less is known about the biological function of *Ovol2* and *Ovol3*.

Ovol2 is expressed in myriad embryonic and postnatal tissues (11, 16). Consistent with a widespread expression pattern, ablation of the *Ovol2* gene results in early embryonic lethality (16), which precludes a comprehensive analysis of its later developmental roles. Interestingly, Ovol2 expression appears to correlate with a proliferative stem/progenitor cell state (16, 17). For instance, Ovol2 protein is detected in the basal layer of skin epidermis (17), where proliferative epidermal stem/progenitor cells reside. Moreover, Ovol2 is strongly expressed in inner cell mass as well as its *in vitro* equivalent, embryonic stem cells (16). The functional significance of Ovol2 expression in proliferating stem/progenitor cells remains to be established.

Mammalian epidermis is an excellent model system to study the molecular circuits that control proliferation and differentiation. Using cultured keratinocytes and mouse models, important regulators of epidermal proliferation and differentiation have been uncovered (18). Among these, c-Myc is the most intriguing because of its multiple and seemingly opposing roles (19). Although c-Myc is expressed in basal cells and clearly important for keratinocyte proliferation, its constitutive overexpression in cultured keratinocytes causes progressively reduced growth, precocious terminal differentiation, and loss of cells that express a high level of β1 integrin, a putative epidermal stem cell marker (20). The latter finding has been interpreted to indicate a c-Myc-stimulated premature exit from the stem cell compartment, a notion that is apparently supported by the observation of decreased $\beta1^{high}$ or label-retaining cells in mice that overexpress c-Myc in the epidermal basal layer (20–22). Notch signaling, which is initiated by ligand binding to the Notch receptor followed by cleavage and nuclear translocation of the intracellular domain that in turn binds to RBP-J to generate a transactivation complex, is critical for terminal differentiation of keratinocytes (19, 23–26). Notch receptors (Notch1, 2, and 3) are not normally expressed in proliferating epidermal

* This work was supported, in whole or in part, by National Institutes of Health Grants R01-AR47320 and K02-AR51482 (to X. D.); R01-AR47320-08S1 (to X. D. and Q. N.); and R01GM75309, R01GM67247, and P50GM76516 (to Q. N.). This work was also supported by National Science Foundation Grant DMS0511169 (to Q. N.).

[S] The on-line version of this article (available at http://www.jbc.org) contains supplemental text, equations, and Figs. S1 and S2.

[1] To whom correspondence should be addressed: Dept. of Biological Chemistry, School of Medicine, D250 Med. Sci. I, University of California, Irvine, CA 92697-1700. Tel.: 949-824-3101; Fax: 949-824-2688; E-mail: xdai@uci.edu.

basal cells, and overexpression of the intracellular domain in these cells promotes a differentiating, spinous cell fate (23). Collectively, these findings suggest that fine-tuning c-Myc expression and suppressing Notch expression/signaling in the basal layer might be important for maintaining a differentiation-refractory progenitor cell state. To date, little is known about molecular mechanisms that directly repress c-Myc and Notch expression in epidermal progenitor cells.

In this work, we use HaCaT keratinocytes to explore the function of Ovol2. We show that Ovol2 regulates independent yet related aspects of keratinocyte proliferation and differentiation, namely suppressing rapid amplification and terminal differentiation but maintaining long term proliferation potential in culture. We present evidence that Ovol2 does so, at least in part, by regulating downstream targets c-*Myc* and *Notch1.*

EXPERIMENTAL PROCEDURES

Cell Culture and Reagents—293T cells (a human kidney epithelial cell line) were maintained in Dulbecco's modified Eagle's medium (Invitrogen) supplemented with 10% fetal bovine serum. UG1 mouse keratinocytes were cultured as previously described (13). HaCaT human keratinocytes were cultured in calcium-free Dulbecco's modified Eagle's medium/Ham's F-12 (3:1) supplemented with 15% fetal bovine serum that had the calcium chelated using Chelex beads (Bio-Rad). The following *Silencer* predesigned siRNAs[2] (Applied Biosystems/Ambion) were used at a concentration of 30–60 nM: Ovol2 #1 (siRNA number 29207) 5′-GGCAUUCGUCCCUACAAAU-3′, Ovol2 #2 (siRNA number 29292) 5′-GGUAUUUCUUAGAGAGAUC-3′, and nontargeting negative control #1 siRNA. The following *Silencer Select* predesigned siRNA (Applied Biosystems/Ambion) was used at a concentration of 10 nM: Ovol2 #3 (siRNA number s33860) 5′-AGAUCGAAAAUCAAGUUCA-3′; and the nontargeting negative control #1. c-Myc inhibitor, 10058-F4 (EMD Biosciences), was used at a concentration of 30 μM and was added to cells 24 h after transfection. DAPT γ-secretase inhibitor (EMD Biosciences) was used at a concentration of 1 μM and was also added 24 h after transfection. For differentiation assays, Ca^{2+} was added at a final concentration of 2.8 mM 72 h after siRNA transfection, and treatment persisted for an additional 4 days.

Nuclear Extracts and Western Blots—Nuclear extracts were made as previously described (27). Protein concentrations were quantified (Bio-Rad protein assay reagent), and equal amounts of protein were run on 10% polyacrylamide gels, followed by transfer to nitrocellulose membranes and probing with antibodies. The following antibodies were used: rabbit anti-Ovol2 (1:250) (16); mouse anti-Rad50 and mouse anti-p84 (1:2000; gift from P. L. Chen, University of California, Irvine); mouse anti-c-Myc (1:250; Santa Cruz Biotechnology); rabbit anti-HDAC1 (1:200; Santa Cruz Biotechnology); rabbit anti-K1, rabbit anti-loricrin, and rabbit anti-K14 (1:2000; gift from J. Segre, National Institute of Health); and mouse anti-β-actin (1:4000, Abcam). The proteins were detected using chemiluminescence (Pierce).

Cell Counts and Clonal Assay—For cell count experiments, HaCaT cells were seeded in triplicate in a 12-well plate and transfected at 20–30% confluence with 60 nM siRNA and Lipofectamine 2000 (Invitrogen) according to manufacturer's instructions. At 24-h intervals spanning 72 h post-transfection, the cells were trypsinized and counted using a hemacytometer. Clonal assays were performed as previously described (28). For first generation clonal assays, HaCaT cells were seeded at 8×10^4 cells/well of a 6-well plate and transfected 24 h later with siRNA. The cells were trypsinized 24 h after transfection (day 2), replated at a density of 500 cells/well in 6-well plates, and retransfected with siRNA on day 8. After 14 days, three of the six wells/sample were fixed in 4% paraformaldehyde for 15 min, washed with 1× PBS, and stained with a solution of 1% Rhodamine B, 1% Nile Blue before washing and air drying. The number and size of colonies were then scored. The remaining three wells were trypsinized, counted, and replated as second generation at a density of 500 cells/well in a 6-well plate.

Immunofluorescence—HaCaT cells were seeded into a 96-well plate and 24 h later transfected with siRNA. Seventy-two hours after transfection, the cells were fixed with 4% paraformaldehyde for 15 min and washed with PBS. Following permeabilization with cold 90% methanol for 5 min at room temperature and PBS washes, the cells were blocked in 10% normal goat serum for 1 h and then incubated with mouse anti-cleaved poly(ADP-ribose) polymerase (Asp^{214}) (1:10; BD Pharmingen) and rat anti-phospho histone H3 (pS28) (1:20; BD Pharmingen) in 1% normal goat serum overnight at 4 °C. The cells were washed with PBS, and the nuclei were stained with 4′,6-diamidino-2-phenylindole. The plates were run on an In-Cell Plate Reader, and the fluorescence was measured using InCell Developer Software.

FACS Analysis—HaCaT cells were seeded in duplicate at 2.5×10^5 cells/10-cm dish and after 24 h were transfected with siRNA. The cells were collected 72 h after transfection. For propidium iodide staining, the cells were washed once with cold PBS, fixed with 70% ethanol for 24 h at −20 °C, followed by two PBS washes. After being stained with a propidium iodide staining solution (50 μg/ml propidium iodide, 0.1% sodium citrate, 0.03% Nonidet P-40, 50 μg/ml RNase A, PBS) for 30 min at room temperature, the cells were then washed once with PBS. For α6 integrin staining, the cells were washed once with 2% fetal bovine serum with PBS and stained on ice for 30 min with a phycoerythrin-conjugated rat anti-CD49f (α6 integrin) antibody (1:40; BD Pharmingen) and the appropriate isotype control. The cells were washed two times with cold PBS, run on a FACS Calibur flow cytometer (BD), and analyzed with FlowJo software (Tree Star Inc.).

Cyclic Amplification of Selected Targets—Cyclic amplification of selected targets was carried out as previously described (3) using purified recombinant His_6-Ovol2 protein. Forty Ovol2-selected clones were sequenced to derive an Ovol2 consensus sequence.

Reporter Assays—Assays were performed in 293T and HaCaT cells. The 293T cells were transfected using calcium phosphate as described (29) and HaCaT cells using Lipo-

[2] The abbreviations used are: siRNA, small interfering RNA; PBS, phosphate-buffered saline; FACS, fluorescence-activated cell sorter; ChIP, chromatin immunoprecipitation; TA, transit amplifying; TGF, transforming growth factor; DAPT, *N*-(*N*-(3,5-difluorophenacetyl)-1-alanyl)-*S*-phenylglycine *t*-butyl ester.

fectamine 2000 (Invitrogen). Typically, transfection experiments were done in 12-well plates with each well transfected with a total of 1.6 μg of plasmids including 0.1 or 0.8 μg (for 293T or HaCaT cells, respectively) of pGL3-c-Myc (4), pGL3-Hes1 (where luciferase is under the control of the *Hes1* promoter; gift from C. C. W. Hughes, University of California, Irvine), or pGL4 Notch1 (where luciferase is under the control of the 2.4-kb *Notch1* promoter; gift from G. P. Dotto, Massachusetts General Hospital (30)), 0.08 or 0.3 μg (for 293T or HaCaT cells, respectively) of β-actin-β-galactosidase construct (transfection control), and varying amounts of pCB6-Ovol2A, an Ovol2A expression vector (as indicated in the figure legends). pCB6+ (empty vector containing the cytomegalovirus promoter) was used as filler DNA. The cells were harvested 24–36 h after transfection, and luciferase activity was measured in whole cell extracts using the luciferase assay system (Promega). β-Galactosidase activity was measured as previously described (31).

Chromatin Immunoprecipitation (ChIP)—HaCaT cells were seeded in 10-cm plates, and each plate was transfected at ~90% confluency with 24 μg of pCB6-Ovol2A using Lipofectamine 2000. The plates were cross-linked 24 h after transfection with 1% formaldehyde for 10 min at room temperature, and chromatin immunoprecipitates were isolated using the ChIP assay kit (Upstate Biotechnology Inc.) and anti-Ovol2 antibody (16) according to the manufacturer's instructions. PCR was performed using human c-Myc primers (4) and human Notch1 primers containing the following sequences: forward, 5′-ACCAGGAGCAGAGGACGTC-3′; and reverse, 5′-CTTTCCTGGCACACCTCTTG-3′. The following PCR program was used: 94 °C for 5 min followed by 31–38 cycles (within the linear range of the primers) of 94 °C for 45 s, 60 °C for 45 s, and 72 °C for 1 min followed by a final extension at 72 °C for 7 min.

Real Time PCR—Total RNA was extracted using TRIzol reagent (Invitrogen) according to the manufacturer's instructions. Five μg of total RNA was reverse transcribed into cDNA using the Superscript III RNase H reverse transcriptase (Invitrogen) according to the manufacturer's instructions. All of the primers used for quantitative real time PCR were designed to span exon-exon borders to minimize the possibility of nonspecific amplification of genomic DNA. The following primers were used for quantitative real time PCR: glyceraldehyde-3-phosphate dehydrogenase forward, 5′-GGCATCCTGGGCTACACTGAG-3′; glyceraldehyde-3-phosphate dehydrogenase reverse, 5′-TGAGGTCCACCACCCTGTTG-3′; c-Myc forward, 5′-TCTCTCCGTCCTCGGATTCTC-3′; c-Myc reverse, 5′-GGAGCCTGCCTCTTTTCCAC-3′; Notch1 forward, 5′-AATGTGGATGCCGCAGTTG-3′; and Notch1 reverse, 5′-CGGTCCATATGATCCGTGATG-3′. Quantitative real time PCRs were performed using iQ SYBR Green Supermix (Bio-Rad) according to the manufacturer's instructions on an iCycler real time quantitative PCR system (Bio-Rad). The thermal profile included 95 °C for 3 min, 40 cycles of denaturation at 95 °C for 10 s and annealing at 63 °C for 1 min with the optics on for fluorescence monitoring. The reactions were run in triplicate and always included a standard curve and no template sample for each primer set as a control for the linear range and nonspecific PCR products, respectively. Glyceraldehyde-3-phosphate dehydrogenase was used to normalize the data. The mean threshold cycle (C_t) for individual reactions was identified using the iCycler IQ sequence analysis software (Bio-Rad).

Three-dimensional Organotypic Culture—Skin equivalents were prepared in 12-well tissue culture inserts (3-μm pore Thinsert; Greiner Bio One) as previously described (32). Briefly, gels (400 μl/insert) were prepared from collagen type I (BD Biosciences) at a final concentration of 2.5 mg/ml and seeded with 3T3 cells at 2.5×10^4 cells/ml. The gels were submerged in Dulbecco's modified Eagle's medium, 10% fetal bovine serum and grown at 37 °C in a humidified, 95% air, 5% CO_2 atmosphere. After 48 h, the gels were released from the side of the insert using a pipette tip and allowed to contract for 5 days. The medium was replaced every 2 or 3 days. 2×10^5 HaCaT cells (either negative control or Ovol2-depleted)/insert were added and allowed to grow for 2 days before being air-lifted and cultured in medium containing 2.8 mM calcium for 10 days. The medium was changed every other day.

Mathematical Modeling—A cell population model consisting of a system of ordinary differential equations was considered (33, 34) (see supplemental text for equations and details of the model). In the system, after each stem cell (N_0 in total) division, the daughter cells have the probability (p_0) to remain a stem cell, or ($1 - p_0$) to become a progenitor (N_1) cell that can undergo a maximum of M divisions before becoming growth arrested (N_{M+1}) cells. For a smaller M, the solution of the system could be explicitly and analytically expressed. For a large M, the system was solved using NDSolve function in Mathematica. The parameter fitting was based on FindFit function of Mathematica.

RESULTS

Loss of Ovol2 Leads to a Transient Increase in Growth and a Loss of Long Term Proliferation—In both mice and humans, a single *Ovol2* gene encodes different protein isoforms with presumably opposing transcriptional regulatory activities (5, 11). We therefore first determined which isoform of Ovol2 is expressed in epidermal keratinocytes. By Western blot analysis of nuclear extracts from mouse and human keratinocytes and mouse skin, we found that based on the sizes of the proteins seen in each of these samples, Ovol2A repressor is the dominant isoform expressed in epidermis *in vivo* and cultured keratinocytes *in vitro* (Fig. 1*A*). The other isoforms, namely Ovol2B and Ovol2C, were not detected under our experimental conditions.

Next we turned to use siRNAs to knockdown Ovol2 in HaCaT human keratinocytes, an immortalized cell line that displays epidermal progenitor cell activity, *i.e.* forming a stratified epidermis under organotypic culture conditions (28, 35, 36). A number of different differentiation-specific markers are expressed in HaCaT cells under organotypic conditions, although stratification is incomplete and imperfect (37). These cells were chosen for our study because in culture they contain a small subset of quiescent stem/progenitor-like cells (28), mimicking epidermal homeostasis *in vivo*. When compared with cells transfected with a negative control siRNA that does not target any known gene, Ovol2 proteins were effectively depleted with *Ovol2*-specific siRNAs, and knockdown persisted

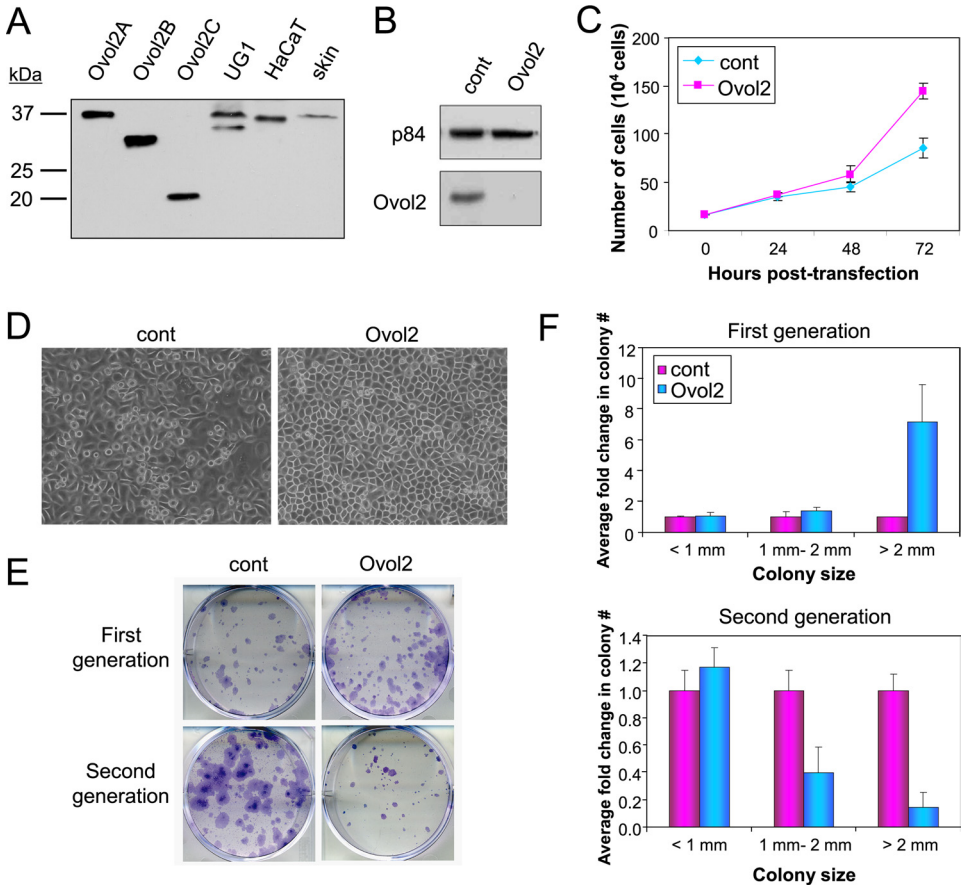

FIGURE 1. **Increased transient growth and decreased long term clonogenicity in Ovol2-depleted keratinocytes.** *A*, Western blot analysis of Ovol2 isoform expression in keratinocytes and skin. Nuclear extracts were made from 293T cells transfected with Ovol2A, Ovol2B, or Ovol2C expression constructs, UG1 mouse keratinocytes, HaCaT cells, and mouse skin. Note that OVOL2A is, as expected, slightly smaller than Ovol2A. The *second band* in UG1 cells is likely a degradation product because its presence varies from experiment to experiment. *B*, Western blot showing efficient siRNA-directed depletion of Ovol2 72 h after transfection. Nuclear protein p84 was used as a loading control (*cont*). *C*, growth curve of short term, high density cultures of control and Ovol2-depleted cells ($n = 3$). *D*, morphology of Ovol2-depleted keratinocytes 72 h after transfection. *E*, clonal analysis of control and Ovol2-depleted keratinocytes. *F*, quantitative analysis of results shown in *E*. Shown are the average values with standard deviations from two independent experiments each with triplicate samples.

in culture for at least 6 days for the most effective siRNA (Fig. 1*B* and supplemental Fig. S1*A*). A growth curve analysis revealed a significantly higher number of cells in Ovol2-depleted high density culture, particularly at 72 h after siRNA transfection (1.7-fold ± 0.12) (Fig. 1*C*). Consistently, the Ovol2 knockdown plates appeared more confluent, and the cells were more tightly packed on the plate than the negative control plates (Fig. 1*D*). Three different siRNA oligonucleotides (Ovol2 #1 targets exons 3 and 4, Ovol2 #2 targets the 3′-untranslated region, and Ovol2 #3 targets exon 2) produced a similar trend, albeit to a lesser extent for the less effective siRNAs #2 and #3 (supplemental Fig. S1, *C* and *D*). This finding suggests that the increase in cell number is not an off target effect. Knockdown was also performed in mouse keratinocytes using adenoviral small hairpin RNA against *Ovol2*, and a similar increase in cell number was observed (data not shown). Subsequent experiments focused on the most effective siRNA (#1) and HaCaT cells.

Because cultured keratinocytes are a heterogeneous population of cells with different proliferation potentials (28, 38, 39), we performed clonal assays in which cells are plated at a clonal density to determine the proliferation potential of individual cells. Specifically, we transfected HaCaT cells with either control or *Ovol2* siRNA at days 1 and 8 to efficiently knockdown Ovol2 during the first 14 days of clonal assay (this we term first generation). We then assessed the proliferation potential of the cells harvested from the first generation by replating a portion of them at a clonal density, but this time with no additional siRNA knockdown (this we term second generation). Consistent with an increased cell number in short term high density cultures described above, we observed a reproducible increase in the number of large (> 2 mm) colonies in Ovol2-depleted first generation cultures when compared with negative control (Fig. 1, *E*, *top panels*, and *F*, and supplemental Fig. S2, *top panel*). Trypan blue staining showed that Ovol2 depletion did not affect the viability of the first generation cells (data not shown). Interestingly, after replating an equal number of first generation cells, we now observed a reduction in both colony size and number in the second generation culture derived from cells that had been previously depleted of Ovol2 (Fig. 1, *E*, *bottom panels*, and *F*, and supplemental Fig. S2, *bottom panel*). This result suggests that depleting Ovol2 leads to a reduction in the number of keratinocytes that possess long term proliferation potential. Together, our results indicate that depletion of Ovol2 results in a transient increase in growth but a decrease in long term proliferation.

Reduced Active Cycling Accompanies the Growth Phenotype of Ovol2-depleted Cells—A priori, an increase in cell number can be caused by a decrease in cell death or an increase in cell proliferation. To distinguish between these possibilities, we stained negative control and Ovol2 knockdown cells cultured under high density conditions for the presence of cleaved poly-(ADP-ribose) polymerase, which symbolizes activated apoptosis (40), and phospho-H3 (pS28), which marks cells in the mitotic phase (specifically the prophase to anaphase transition) of the cell cycle (41). A slight decrease in the number of cleaved poly(ADP-ribose) polymerase positive cells was observed in Ovol2 knockdown cells (0.17% ± 0.03) when compared with negative control cells (0.25% ± 0.07) (Fig. 2, *A* and *B*, *left columns*). This slight change is consistent with, but unlikely to completely account for the increase in cell number. Contradictory to our prediction, there was a significant decrease in the

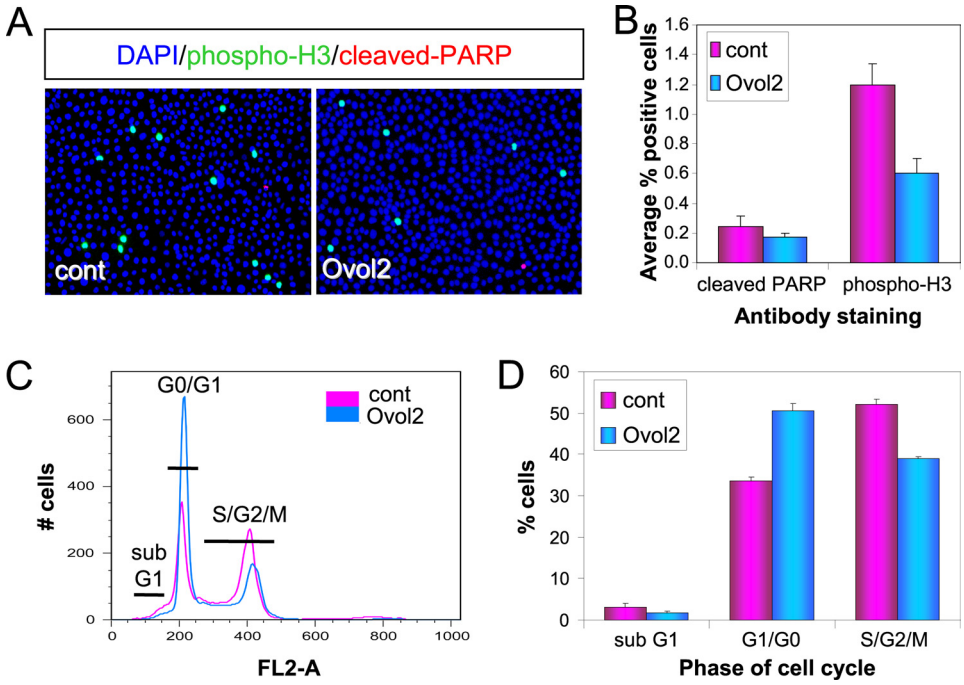

FIGURE 2. **Decreased apoptosis and reduced active cycling accompany the growth phenotype of Ovol2 knockdown cells.** HaCaT cells were transfected with either negative control (*cont*) or *Ovol2* siRNA and then used for analysis 72 h post-transfection. *A*, immunofluorescence of cells stained with anti-cleaved poly(ADP-ribose) polymerase (*red*) and anti-phospho-H3 (*green*). 4′,6-Diamidino-2-phenylindole (*DAPI*) was used to stain the nuclei (*blue*). *B*, quantitative analysis of experiments in *A* reveals a slight reduction of apoptotic cells (*left*) and a significant reduction of mitotic cells (*right*) in Ovol2-depleted culture. The results are from a total of five samples from two independent experiments. *C*, representative histogram of cell cycle profiles. Note the increase in G_1 population and concurrent decrease in $S/G_2/M$ population in Ovol2 knockdown samples. *D*, average percentage of sub-G_1, G_1/G_0, and $S/G_2/M$ cells in control and Ovol2-depleted culture, as calculated from three samples each from two independent experiments.

number of phospho-H3-positive cells in Ovol2 knockdown cells (average of 2-fold change ± 0.24) (Fig. 2, *A* and *B*, *right columns*). An overall reduction in the number of actively cycling cells was confirmed by FACS analysis of cell cycle profiles, revealing a 34% increase in G_1/G_0 cells and a 25% decrease in $S/G_2/M$ cells in the Ovol2-depleted high density culture (Fig. 2, *C* and *D*). Again, a slight reduction in apoptotic cells, as monitored by the sub-G_1 population, was observed.

Mathematic Modeling Suggests That Ovol2 Suppresses the Rate of Keratinocyte Cycling but Prolongs the Number of Divisions They Undergo—To explore the cellular basis of these seemingly contradictory observations, we applied a simple cell lineage mathematic model (33, 34) to examine keratinocyte stem/progenitor cell evolution. We considered three distinct cell types (42): slow cycling stem cells that can proliferate indefinitely, faster cycling progenitor cells with a set proliferation potential (indicated by M number of cell divisions they are able to undergo), and growth-arrested cells (Fig. 3*A*). Using this model, we explored various parameters that would allow the recapitulation of our experimental observations. We found that a total of 36 rounds of progenitor cell divisions are necessary to mimic the observed growth of normal HaCaT keratinocytes (data not shown). Under this precondition, we found that decreasing t_1 (cell cycle time for progenitor cells) but not t_0 (cell cycle time for stem cells) was necessary to robustly capture the Ovol2 depletion-induced transient increase in proliferation in high density culture (Fig. 3*B*, *left panel*). However, this could not replicate the finding of decreased clonogenicity in second generation Ovol2 knockdown culture (Fig. 3*B*, *right panel*). Importantly, using a smaller M in addition to decreasing t_1 recapitulated both the increased growth in high density culture and the decreased clonogenicity in second generation culture of Ovol2-depleted cells (Fig. 3*C*). In contrast, decreasing p_0 had minimal impact on the growth behavior of Ovol2-depleted cells regardless of whether M was reduced or not (Fig. 3*C* and data not shown). These results suggest that both decreased cell cycle time and compromised proliferation potential of progenitor cells are critical for the observed growth phenotype of Ovol2-deficient culture. Indeed, we observed a remarkable decrease in the expression of α6 integrin, which when highly expressed, marks keratinocytes that possess long term proliferation potential and increased clonogenecity (43, 44), in Ovol2 knockdown cells (Fig. 3*D*). This result provides further correlative support that Ovol2 is required for cultured keratinocytes to maintain their proliferation potential.

Ovol2 Suppresses Active Keratinocyte Proliferation by Repressing c-Myc Expression—How does Ovol2 keep keratinocytes proliferation in check? We entertained the possibility that Ovol2 might function by directly repressing a positive regulator of the cell cycle. c-Myc is an excellent candidate because 1) it is repressed by Ovol1, whose zinc finger domain is highly homologous to that of Ovol2 (11, 13); and 2) its expression level in keratinocytes has been proposed to govern whether a stem cell should exit into the transit amplification (TA) stage, how well a TA cell proliferates, or whether it should terminally differentiate (20–22, 45, 46).

We first examined c-*Myc* expression in control and Ovol2 knockdown cells. Loss of Ovol2 indeed caused an up-regulation of both c-*Myc* mRNA and c-Myc protein levels (Fig. 4, *A* and *B*). Next we asked whether inhibiting c-Myc activity might rescue the growth phenotype of Ovol2 knockdown cells. A small molecule inhibitor (10058-F4) that interferes with c-Myc binding to its partner in transcriptional activation (47) was added to keratinocytes cultured under clonal conditions with or without Ovol2 knockdown. At an inhibitor concentration where minimal change of colony growth was observed in first generation control cultures, Ovol2 knockdown no longer elicited a significant increase in transient proliferation (Fig. 4, *C* and *D*). In contrast, Ovol2 knockdown still resulted in a dramatic reduction of colony

formation in second generation cultures regardless of whether the c-Myc inhibitor was present or not (data not shown). Consistent with this finding, addition of the c-Myc inhibitor was unable to rescue the loss of $\alpha6^{high}$ cells caused by Ovol2 depletion (Fig. 4*E*). Collectively, these results suggest that c-Myc up-regulation accounts at least in part for the Ovol2 depletion-induced transient increase in proliferation but not for the loss of long term proliferation potential.

We next asked whether c-*Myc* is a direct target of Ovol2. Cyclic amplification of selected targets analysis revealed an Ovol2 consensus DNA-binding sequence that is almost identical to the Ovol1 cognate sequence (3) (Fig. 5*A*). Because a conserved Ovol1 consensus was previously discovered in a 1.6-kb c-*Myc* promoter fragment to mediate Ovol1 repression (4), we performed reporter assays to ask whether Ovol2 also represses the c-*Myc* promoter. Transfection of an Ovol2A-expressing construct repressed the promoter-driven luciferase activity in a dose-dependent manner (Fig. 5*B*), whereas transfection of a construct expressing Ovol2B or Ovol2C that lacks the functional SNAG repressor domain had no effect (data not shown). When the Ovol consensus binding site was deleted or mutated, repression by Ovol2A was reduced but not abolished (Fig. 5*B*), suggesting the presence of additional, noncanonical Ovol2A-responsive element(s). Indeed, a minimal c-*Myc* promoter that contains only 100 bp upstream (proximal region) of the transcriptional start site (4) was repressed by Ovol2A in both 293T and HaCaT cells (Fig. 5*C*). This region does not contain any Ovol2 consensus but contains recognition sequences for Smad3 and E2F that mediate transcriptional repression (48–50). Although mutation of the Smad3-binding sequence had no negative effect, mutation of the E2F-binding sequence significantly compromised repression by Ovol2A (Fig. 5*D* and data not shown). In ChIP assays, Ovol2 was found to occupy both the distal consensus site and the proximal noncanonical site of the endogenous c-*Myc* promoter, with binding to the noncanonical site being significantly more prominent (Fig. 5*E*). Taken together, our findings demonstrate that Ovol2A represses c-*Myc* expression via direct binding to the c-*Myc* promoter.

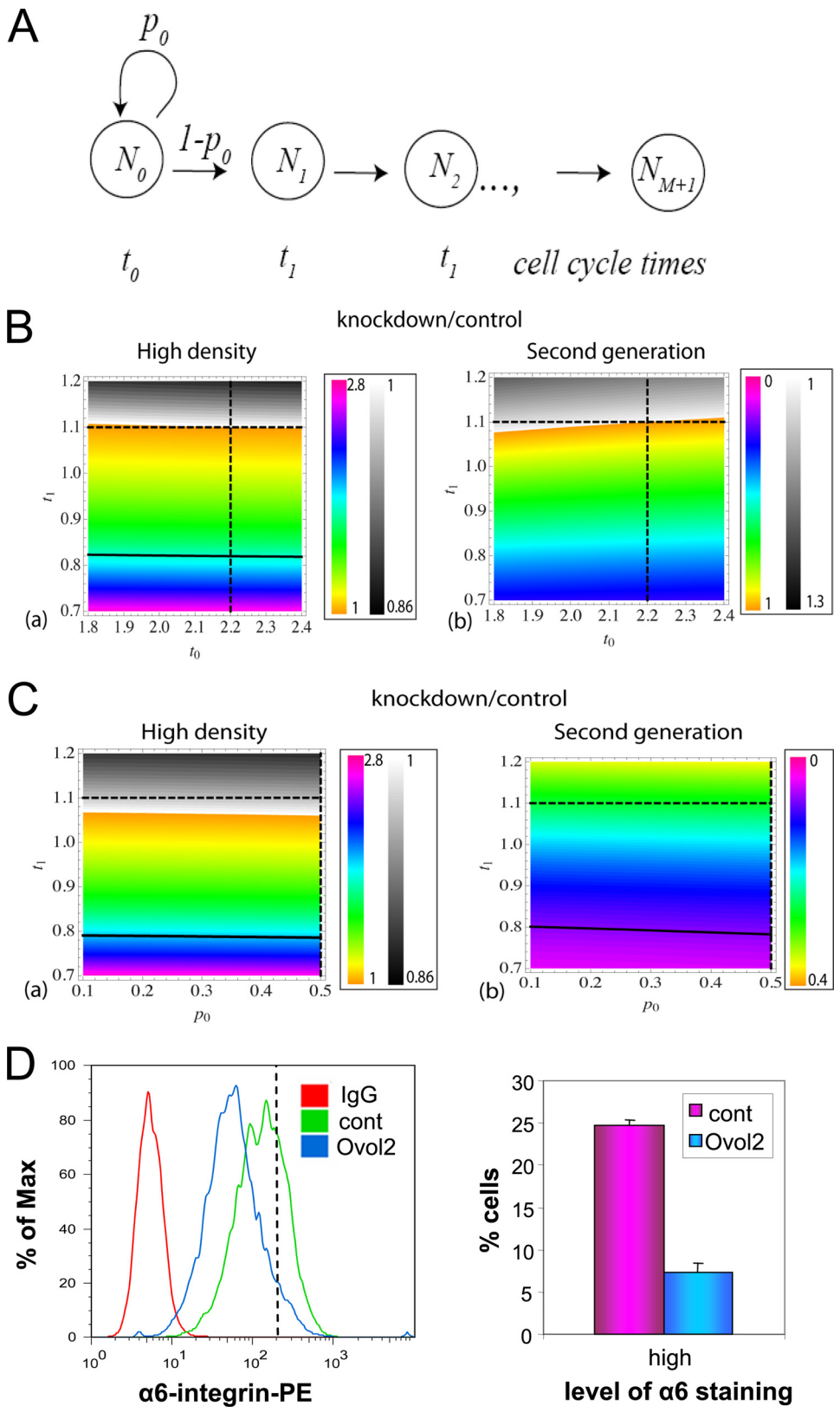

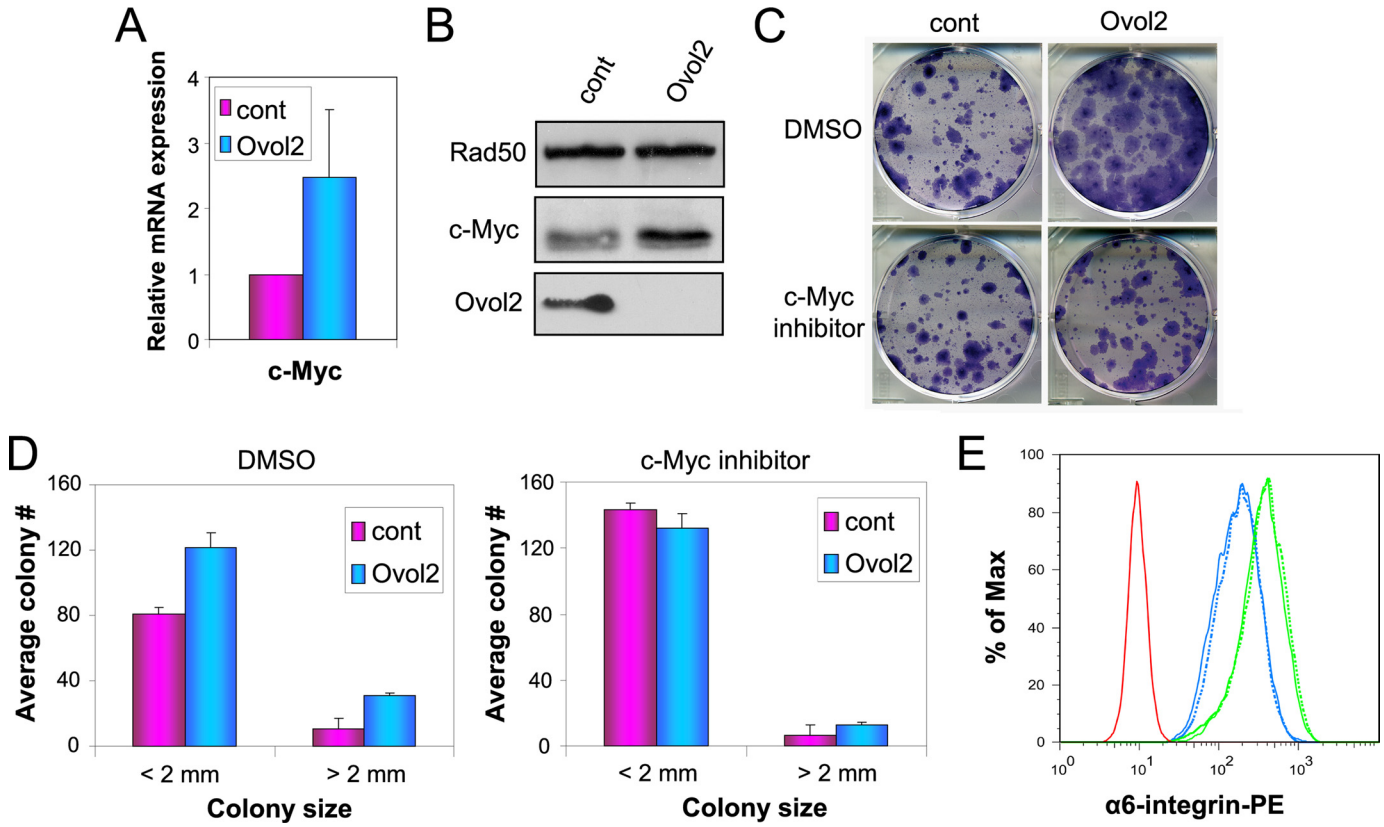

FIGURE 4. **Up-regulated c-*Myc* expression in Ovol2-depleted cells and rescue of their transient growth by a c-Myc inhibitor.** *A* and *B*, increased c-*Myc* mRNA (*A*) ($n = 3$) and protein production (*B*) in the absence of Ovol2 72 h after transfection. cDNA in quantitative real time PCR was normalized using glyceraldehyde-3-phosphate dehydrogenase. For the Western blot, Rad50 was used as a loading control (*cont*) for the nuclear extracts. *C* and *D*, results of first generation clonal assays in the presence of dimethyl sulfoxide (*DMSO*) (vehicle control) or 30 μM c-Myc inhibitor. The inhibitor was present for the entire duration of the first generation culture. Representative plate images are shown in *C*, and quantitative analysis is shown in *D*. The average values with standard deviations were calculated from triplicate samples in a single experiment, and the results are representative of two independent experiments. *E*, representative histogram of FACS analysis of α6 integrin (CD49f)-stained cells 72 h after transfection (two independent experiments each with duplicate samples). The *solid* and *dotted lines* indicate samples that are treated with dimethyl sulfoxide and the c-Myc inhibitor, respectively. *Red*, isotype control; *green*, control siRNA; *blue*, *Ovol2* siRNA.

Ovol2 Suppresses Keratinocyte Terminal Differentiation by Repressing Notch1—The growth and differentiation of keratinocytes are tightly linked. To test whether Ovol2 depletion predisposes keratinocytes to terminal differentiation, we treated negative control and Ovol2 knockdown cells with TGF-β or calcium to induce growth arrest or terminal differentiation, respectively, and examined the expression of keratin 1 (K1) and loricrin, markers of terminal differentiation. Neither Ovol2 knockdown or TGF-β treatment alone was sufficient to induce K1 and loricrin expression (Fig. 6*A*). However, TGF-β was able to induce loricrin expression when Ovol2 was depleted. Moreover, induction of K1 and loricrin expression by calcium treatment was significantly more remarkable in Ovol2-depleted cells. The up-regulation of differentiation markers was also seen for *Ovol2* siRNAs #2 and #3 (supplemental Fig. S1*E*), indicating that the premature differentiation is not an off target effect. To mimic conditions *in vivo*, we next turned to a three-dimensional organotypic culture system. Control or Ovol2-depleted HaCaT keratinocytes were grown on a fibroblast-collagen matrix under conditions that allowed the examination of early differentiation and stratification events. At a culturing time point when control samples showed expression of basal marker K14 but no detectable expression of differentiation marker K1 (51), Ovol2-depleted samples stained weakly for K14 but strongly for K1 (Fig. 6*B*). Collectively, our results suggest that Ovol2 suppresses the differentiation tendency of keratinocytes; in its absence, keratinocytes are more prone to extracellular signal-induced terminal differentiation.

Notch signaling plays a pivotal role in promoting keratinocyte differentiation. We therefore wondered whether this sig-

FIGURE 3. **Increased proliferation rate and decreased proliferation potential of Ovol2-depleted keratinocytes.** *A*, a schematic diagram of keratinocyte stem cell evolution in culture. N_0, number of stem cells; N_1 to N_M, number of progenitor cells; N_{M+1}, number of growth arrested cells; p_0, probability of the daughter cells of a stem cell to remain a stem cell; *M*, number of progenitor cell divisions; t_0 and t_1, cell cycle times of a stem and a progenitor cell, respectively. *B*, the effects of varying t_0 and t_1 on cell number (ratio between knockdown and control cells) when $p_0 = 0.5$ and $M = 36$. The *solid black line* in high density cultures (*panel a*) shows the expected ratio based on experimental data; note the absence of black line in second generation culture (*panel b*). The values set for control keratinocytes are marked by *dotted black lines*. *C*, the effects of varying t_1 and p_0 on cell number when $M = 20$. Note the presence of *black lines* (fitting to experimental data) in both high density (*panel a*) and second generation (*panel b*) cultures irrespective of varying p_0. *D*, FACS analysis using anti-α6 integrin-phycoerythrin (CD49f) antibody 72 h after transfection. Shown on the *left* are representative profiles from a single experiment, and the average values of three samples each from two independent experiments are shown on the *right*. The cut-off value used for quantitative analysis is indicated by the *dotted line*, with cells to the *right* of the line being scored as $\alpha6^{high}$ and those to the *left* being scored as $\alpha6^{low}$. *cont*, control.

A

Position	1	2	3	4	5	6	7	8	9	10
A (%)	65	55	73	40	18	0	8	18	93	23
C (%)	3	0	0	58	37	0	12	2	2	15
G (%)	20	15	5	2	0	100	0	0	0	12
T (%)	12	30	22	0	45	0	80	80	5	50
Ovol2 consensus	A	A/T	A/T	C/A	T/C	G	T	T	A	T/A
Ovol1 consensus	A/T	A/T	A/T	C	C/T	G	T	T	A	T/A

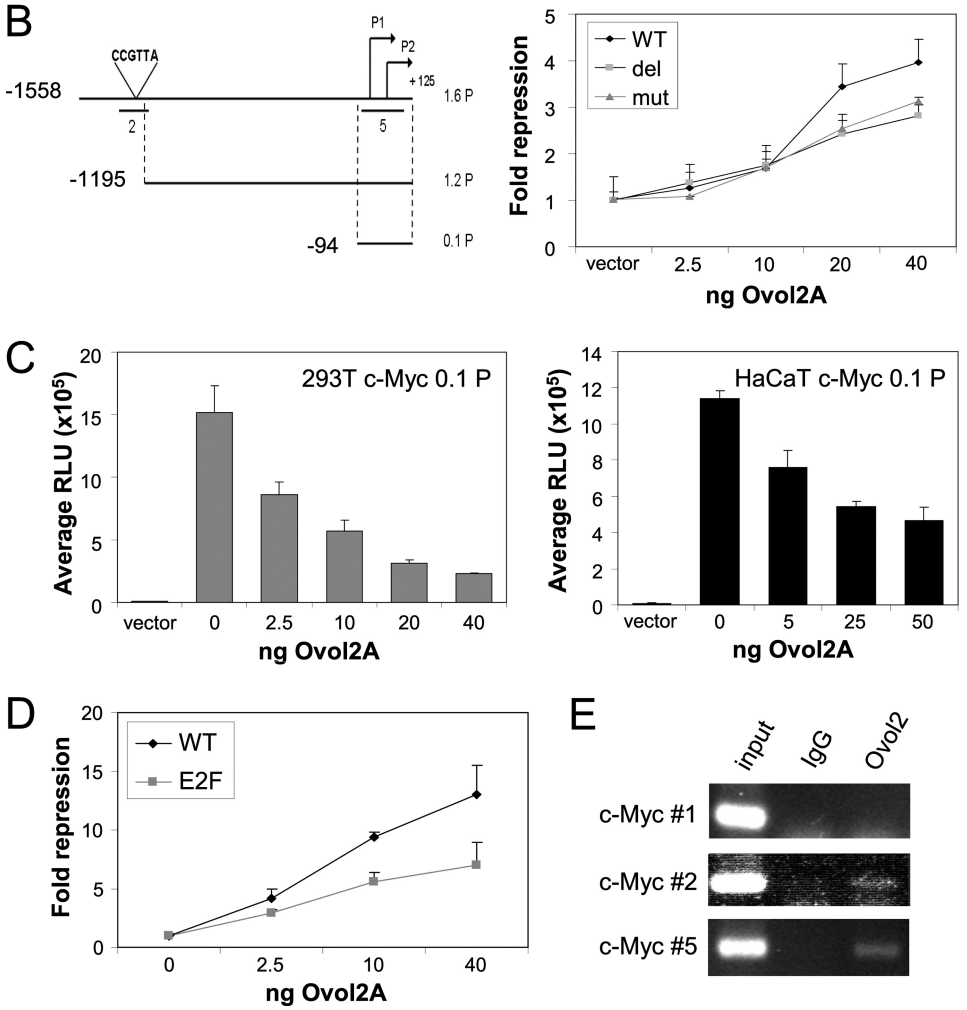

FIGURE 5. **Ovol2 directly represses c-*Myc*.** *A*, result of cyclic amplification of selected targets analysis revealing an Ovol2 binding consensus, which is compared with the known Ovol1 binding consensus (4). *B*, *left panel*, diagram (adapted from Ref. 4) of the human c-*Myc* promoter in plasmid 1.6 P (wild type pGL3-c-Myc) and in the deletion constructs 1.2 P-del and 0.1 P. Transcription start sites are indicated as P1 and P2. *Right panel*, repression of 1.6 P wild type and mutant promoters containing deletion (1.2 P-del) and point mutations (1.6 P-mut) of the CCGTTA Ovol2 consensus binding site in 293T cells. *C*, Ovol2 represses the c-*Myc* minimal promoter (0.1 P) lacking any Ovol2 consensus. Shown are reporter assays in 293T (*left panel*) and HaCaT (*right panel*) cells. *RLU*, relative luciferase unit. *D*, Ovol2 repression of the minimum promoter requires the presence of an E2F-binding site. Each *bar* represents the average of triplicate samples in a single experiment, and the results are representative of multiple experiments ($n = 3$). The *error bars* are the standard deviations of triplicate samples. Luciferase activities were normalized for transfection efficiency by using a *β-actin* promoter driving lacZ as an internal control. *E*, ChIP assays showing Ovol2 binding to both the distal consensus (site 2) and proximal nonconsensus regions (site 5) in the c-*Myc* promoter. See *B* for ChIP primer positions. An upstream region of the c-*Myc* promoter (outside of 1.6 P) was used as a control for nonspecific binding of Ovol2 (site 1). *WT*, wild type.

naling pathway is affected by the loss of Ovol2. Examination of our microarray data (to be published else where) revealed a 1.9-fold increase in *Notch1* transcript levels in Ovol2-depleted keratinocytes, whereas no change was seen for other *Notch* genes. Real time PCR confirmed *Notch1* up-regulation at 24, 48, and 72 h after transfection of *Ovol2* siRNA (Fig. 6*C* and data not shown). Consistent with this finding, we found that Ovol2A was able to repress the *Notch1* promoter in a dose-dependent manner in both 293T and HaCaT cells (Fig. 6*D*). ChIP analysis showed that Ovol2 bound to the endogenous *Notch1* promoter (Fig. 6*E*), suggesting that Notch1 is a direct target of Ovol2. Moreover, the promoter activity of *Hes1*, a known target of Notch signaling (52), was repressed by Ovol2A in a dose-dependent manner (Fig. 6*F*). These results demonstrate that Ovol2 modulates Notch1 expression and downstream signaling.

To address the importance of Notch 1 in the role of Ovol2 in regulating differentiation competence, we repeated the calcium induction experiment, this time including DAPT, a γ-secretase inhibitor that blocks Notch signaling (53, 54). The induction in K1 expression by the loss of Ovol2 was completely abolished when DAPT was added (Fig. 6*G*). Different concentrations of DAPT were used and yielded similar findings (data not shown). In contrast, blocking Notch signaling did not rescue Ovol2 depletion-induced loss of long term colony formation (data not shown). Therefore, we conclude that Ovol2 normally suppresses Notch signaling to prevent premature terminal differentiation of keratinocyte progenitor cells.

DISCUSSION

Our study has elucidated an important function for Ovol2 in human epidermal keratinocyte growth and differentiation. We have shown that Ovol2 regulates three related cellular aspects: proliferation rate, proliferation potential, and differentia-

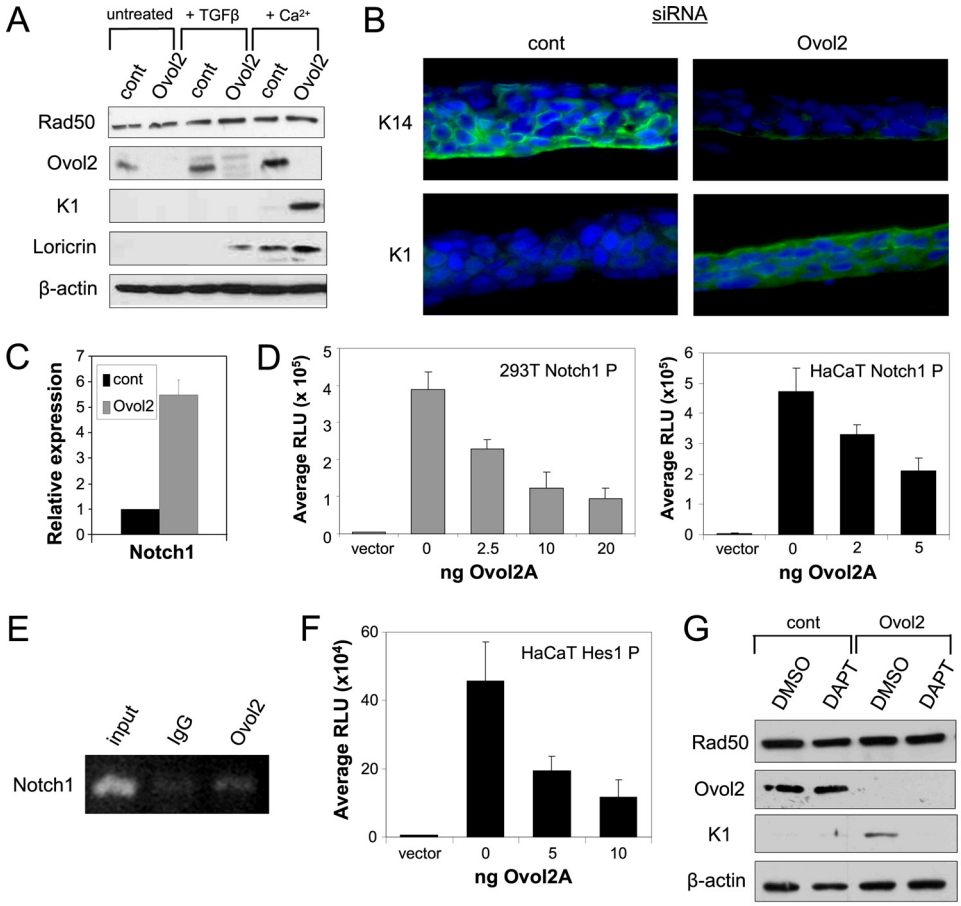

FIGURE 6. **Up-regulated *Notch1* expression in Ovol2-depleted cells and rescue of their accelerated differentiation by Notch signaling inhibitor DAPT.** *A*, HaCaT cells were transfected with either negative control (*cont*) or *Ovol2* siRNA and 72 h post-transfection were treated with either TGF-β or Ca^{2+} to induce growth arrest or terminal differentiation, respectively. Western blots were performed to examine the expression of K1 and Loricrin. *B*, representative results of three-dimensional culture to show that Ovol2 depletion leads to precocious K1 expression. *C*, Ovol2 knockdown cells show elevated *Notch1* mRNA expression 72 h after transfection ($n = 3$). *D*, Ovol2 represses the *Notch1* promoter in both 293T cells (*left panel*) and HaCaT cells (*right panel*). See legend to Fig. 5 for more information. *E*, ChIP assay showing that Ovol2 binds to the *Notch1* promoter. The upstream region of the c-*Myc* promoter (Fig. 5*D*, site 1) was used as a negative control. *F*, Ovol2 represses the *Hes1* promoter in HaCaT cells. *G*, differentiation assay was performed as in *A*, except that dimethyl sulfoxide (*DMSO*) or DAPT was added to the cells before differentiation; shown are Ca^{2+}-treated samples.

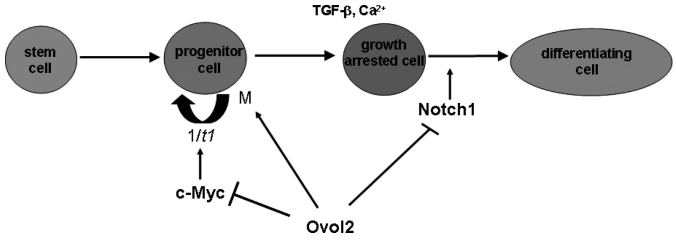

FIGURE 7. **Working model of Ovol2 function in keratinocyte growth and differentiation.** The *arrows* indicate positive regulation, whereas *blunted lines* indicate negative regulation.

tion tendency (Fig. 7). In doing so, Ovol2 contributes to the overall genetic program that maintains keratinocytes in a proliferation-competent and differentiation-resistant state, that of a stem/progenitor cell.

Balancing Cell Cycling with Long Term Proliferation Potential in a Single Progenitor Cell Population: Role of Ovol2—Loss of Ovol2 leads to an initial transient increase in growth but decreased long term clonogenicity. Similar cellular changes have been reported for keratinocytes deficient for Rac1 or overexpressing c-Myc (20–22, 55–57). In a widely accepted model of epidermal homeostasis, it is posited that stem cells that reside in the epidermal basal layers divide infrequently to give rise to TA cells that cycle faster but are destined to terminally differentiate after a few rounds of cell divisions (42). In the framework of this model, the growth phenomenon of c-Myc- and Rac1-altered cells has been explained by a differential effect of these genes on the different cell type populations present in a heterogeneous keratinocyte culture. One might envision that exit of the so-called stem cells from a slow cycling state will increase the percentage of actively cycling TA cells, thereby resulting in a transient burst in growth. However, because the number of cell divisions that a TA cell can undergo is limited (58), this will ultimately cause a depletion of cells with long term proliferation potential. In an alternative model, misregulation of these genes might affect a single population of progenitor cells, making them cycle faster, thereby exhausting the number of cell divisions that they are programmed to undergo. Our mathematic modeling of the behavior of control and Ovol2-depeted keratinocytes presents a scenario that is more consistent with the second model. Reducing the cell cycle time (t_1) and proliferation potential (M) of the progenitor cell population indeed can recreate the observed increase in transient growth and decrease in colonogenicity, whereas changing the cell cycle time (t_0) and/or exit probability (p_0) of a slow cycling stem cell population cannot. From this analysis, we infer that although there clearly is heterogeneity in terms of proliferation rate (slow cycling *versus* fast cycling) in cultured keratinocytes, such heterogeneity may not be functionally relevant to the growth of these cells. This said, it is important to note that our modeling was done using previously described experimental parameters, namely that ~10% of cultured HaCaT keratinocytes are slow cycling stem cells and that these stem cells cycle at a rate that is half of the TA cells (28). These constraints dictate that the rare presence of slow cycling stem cells generates a minimal impact on overall culture growth.

In principle, our findings are consistent with the recently proposed model that a single population of proliferating progenitor cells is sufficient to maintain normal homeostasis of mouse tail epidermis (42, 59, 60) and suggest that the same might be true for cultured human keratinocytes. More impor-

tantly, our studies uncover an important novel player, transcription factor Ovol2, that regulates the cellular activities of keratinocytes. If a normal progenitor cell has an intrinsically set number of cell cycles that they can undergo (*i.e.* a set proliferation potential), then when cycling faster (decreasing t_1), they will exit the cell cycle faster. This calls for means that keep proliferation rate in check to achieve populational longevity. Moreover, any molecular alterations that minimize this proliferation potential (*i.e.* decreasing *M*) will cause premature growth arrest. It is likely that both mechanisms (proliferation rate and potential) account for the observed reduction in the number of total cycling cells as well as long term clonogenicity in Ovol2-depleted culture. As such, our combinatory experimental and modeling approach sets a useful paradigm to study the function of other critical regulators of stem/progenitor cell homeostasis in epidermis as well as in other tissues.

Molecular Mechanism of Ovol2 Function in Controlling Keratinocyte Proliferation—Consistent with the finding of similar phenotypes caused by Ovol2 depletion and c-Myc overexpression, our results demonstrate that c-Myc up-regulation accounts for the transiently increased proliferation in Ovol2 knockdown cells. However, inhibiting c-Myc function in these cells is not sufficient to rescue the loss of long term proliferation potential. These data corroborates our modeling finding that Ovol2 independently regulates proliferation rate and proliferation potential. Although its role in the proliferation rate control is in part mediated by repressing c-*Myc* expression, Ovol2 must regulate additional molecular events to control proliferation potential.

The finding that Ovol2, like Ovol1, also represses c-*Myc* is intriguing. Ovol1 is predominantly expressed in suprabasal cells, whereas Ovol2 is predominantly expressed in basal cells. However, our previous analysis of *Ovol1*/*Ovol2* compound mutants has provided evidence for possible functional redundancy and compensation between the two *Ovol* genes in an *in vivo* setting (17). Sharing a common molecular target offers a partial explanation for this observation. Importantly, despite regulating a common target, depletion of the two Ovol proteins leads to apparently opposite cell biological outcomes because of their different sites of expression: loss of Ovol1 results in expansion of late epidermal progenitor cells, whereas loss of Ovol2 results in depletion of long term proliferating keratinocytes. This further highlights the importance of intricate c-Myc regulation at multiple stages of keratinocyte progenitor cell evolution: down-regulation of c-Myc is important for both keeping a long-lived progenitor cell population and initiating postmitotic differentiation (19). Further studies are now necessary to examine whether Ovol2 is also required for maintaining epidermal progenitor cells *in vivo*.

Another interesting finding of our study is that Ovol2 is able to repress transcription via an E2F-binding sequence. We have previously shown that Ovol1 also represses the c-*Myc* minimal promoter, where this E2F site resides (4). It is possible that DNA binding via an E2F protein underlies both Ovol1 and Ovol2 repression of c-*Myc*. A likely candidate is E2F4/5, which is known to form a repressor complex with Smad3 and p107 to repress c-*Myc* expression (48–50). Additional studies are needed to test this notion.

Ovol2, Notch1, and Keratinocyte Differentiation—Our work highlights a role for Ovol2 in negatively modulating terminal differentiation of keratinocytes even when differentiation-inducing signals are present. However, when such signals are absent, the loss of Ovol2 alone is insufficient to trigger differentiation, suggesting that Ovol2 is not a master switch of differentiation but instead regulates differentiation competence. We have shown that Ovol2 performs this function by repressing *Notch1* expression as well as downstream signaling. Previous studies have underscored the importance of down-regulating Notch signaling in basal progenitor cells to prevent premature spinous cell differentiation (23) and shown that epidermal growth factor receptor signaling negatively regulate *Notch1* transcription. While epidermal growth factor receptor repression of *Notch1* is via an indirect mechanism that involves tumor suppressor p53 (30), we have found *Notch1* to be a direct transcriptional target of Ovol2. Together, these findings indicate that multiple mechanisms are in place to repress *Notch1* expression and activity in the proliferating epidermal progenitor cells.

The ability to suppress differentiation is conceivably very important for normal tissue progenitor cells to maintain a differentiation-resistant state, but this ability, when hijacked by malignant cells, can lead to differentiation refractory tumor growth. In fact aberrant epidermal growth factor receptor signaling is frequently linked to tumorigenesis. Importantly, Ovol2 not only suppresses terminal differentiation but also poses a limit on the rate of proliferation in keratinocyte progenitor cells. This may be significant for developmental progenitor cells to maintain an undifferentiated state while restricting unwanted growth. Studies of tissue-specific knock-out mouse models are ongoing to examine whether the same holds true *in vivo*.

Acknowledgments—We thank Julie Segre for α-K14, α-K1, and α-loricrin antibodies; Phang-Lang Chen for α-p84 and α-Rad50 antibodies; Renu Roy for assistance with the organotypic cultures; Dawoud Sulaiman, Ashley Brown, and Tiffany Price for counting colonies; G. Paolo Dotto for the Notch1 promoter construct; Chris Hughes for the Hes1 promoter construct; and Joan Massague for the mutant c-Myc promoter-luciferase constructs that lack E2F- and Smad3-binding sites.

REFERENCES

1. Andrews, J., Garcia-Estefania, D., Delon, I., Lü, J., Mével-Ninio, M., Spierer, A., Payre, F., Pauli, D., and Oliver, B. (2000) *Development* **127,** 881–892
2. Li, B., Nair, M., Mackay, D. R., Bilanchone, V., Hu, M., Fallahi, M., Song, H., Dai, Q., Cohen, P. E., and Dai, X. (2005) *Development* **132,** 1463–1473
3. Nair, M., Bilanchone, V., Ortt, K., Sinha, S., and Dai, X. (2007) *Nucleic Acids Res.* **35,** 1687–1697
4. Nair, M., Teng, A., Bilanchone, V., Agrawal, A., Li, B., and Dai, X. (2006) *J. Cell. Biol.* **173,** 253–264
5. Unezaki, S., Nishizawa, M., Okuda-Ashitaka, E., Masu, Y., Mukai, M., Kobayashi, S., Sawamoto, K., Okano, H., and Ito, S. (2004) *Gene* **336,** 47–58
6. Mével-Ninio, M., Terracol, R., Salles, C., Vincent, A., and Payre, F. (1995) *Mech. Dev.* **49,** 83–95
7. Oliver, B., Singer, J., Laget, V., Pennetta, G., and Pauli, D. (1994) *Development* **120,** 3185–3195

8. Payre, F., Vincent, A., and Carreno, S. (1999) *Nature* **400,** 271–275
9. Chidambaram, A., Allikmets, R., Chandrasekarappa, S., Guru, S. C., Modi, W., Gerrard, B., and Dean, M. (1997) *Mamm. Genome* **8,** 950–951
10. Dai, X., Schonbaum, C., Degenstein, L., Bai, W., Mahowald, A., and Fuchs, E. (1998) *Genes Dev.* **12,** 3452–3463
11. Li, B., Dai, Q., Li, L., Nair, M., Mackay, D. R., and Dai, X. (2002) *Genomics* **80,** 319–325
12. Masu, Y., Ikeda, S., Okuda-Ashitaka, E., Sato, E., and Ito, S. (1998) *FEBS Lett.* **421,** 224–228
13. Li, B., Mackay, D. R., Dai, Q., Li, T. W., Nair, M., Fallahi, M., Schonbaum, C. P., Fantes, J., Mahowald, A. P., Waterman, M. L., Fuchs, E., and Dai, X. (2002) *Proc. Natl. Acad. Sci. U.S.A.* **99,** 6064–6069
14. Kowanetz, M., Valcourt, U., Bergström, R., Heldin, C. H., and Moustakas, A. (2004) *Mol. Cell. Biol.* **24,** 4241–4254
15. Descargues, P., Sil, A. K., Sano, Y., Korchynskyi, O., Han, G., Owens, P., Wang, X. J., and Karin, M. (2008) *Proc. Natl. Acad. Sci. U.S.A.* **105,** 2487–2492
16. Mackay, D. R., Hu, M., Li, B., Rhéaume, C., and Dai, X. (2006) *Dev. Biol.* **291,** 38–52
17. Teng, A., Nair, M., Wells, J., Segre, J. A., and Dai, X. (2006) *Biochim. Biophys. Acta* **1772,** 89–95
18. Watt, F. M., Lo Celso, C., and Silva-Vargas, V. (2006) *Curr. Opin. Genet. Dev.* **16,** 518–524
19. Watt, F. M., Frye, M., and Benitah, S. A. (2008) *Nat. Rev. Cancer* **8,** 234–242
20. Gandarillas, A., and Watt, F. M. (1997) *Genes Dev.* **11,** 2869–2882
21. Arnold, I., and Watt, F. M. (2001) *Curr. Biol.* **11,** 558–568
22. Waikel, R. L., Kawachi, Y., Waikel, P. A., Wang, X. J., and Roop, D. R. (2001) *Nat. Genet.* **28,** 165–168
23. Blanpain, C., Lowry, W. E., Pasolli, H. A., and Fuchs, E. (2006) *Genes Dev.* **20,** 3022–3035
24. Moriyama, M., Durham, A. D., Moriyama, H., Hasegawa, K., Nishikawa, S., Radtke, F., and Osawa, M. (2008) *Dev. Cell* **14,** 594–604
25. Rangarajan, A., Talora, C., Okuyama, R., Nicolas, M., Mammucari, C., Oh, H., Aster, J. C., Krishna, S., Metzger, D., Chambon, P., Miele, L., Aguet, M., Radtke, F., and Dotto, G. P. (2001) *EMBO J.* **20,** 3427–3436
26. Fuchs, E., and Raghavan, S. (2002) *Nat. Rev. Genet* **3,** 199–209
27. Schreiber, E., Matthias, P., Müller, M. M., and Schaffner, W. (1989) *Nucleic Acids Res.* **17,** 6419
28. Wan, H., Yuan, M., Simpson, C., Allen, K., Gavins, F. N., Ikram, M. S., Basu, S., Baksh, N., O'Toole, E. A., and Hart, I. R. (2007) *Stem Cells* **25,** 1286–1297
29. Pear, W. S., Nolan, G. P., Scott, M. L., and Baltimore, D. (1993) *Proc. Natl. Acad. Sci. U.S.A.* **90,** 8392–8396
30. Kolev, V., Mandinova, A., Guinea-Viniegra, J., Hu, B., Lefort, K., Lambertini, C., Neel, V., Dummer, R., Wagner, E. F., and Dotto, G. P. (2008) *Nat. Cell. Biol.* **10,** 902–911
31. Eustice, D. C., Feldman, P. A., Colberg-Poley, A. M., Buckery, R. M., and Neubauer, R. H. (1991) *BioTechniques* **11,** 739–743
32. Margulis, A., Zhang, W., and Garlick, J. A. (2005) *Methods Mol. Biol.* **289,** 61–70
33. Lander, A. D., Gokoffski, K. K., Wan, F. Y., Nie, Q., and Calof, A. L. (2009) *PLoS Biol.* **7,** e15
34. Lo, W. C., Chou, C. S., Gokoffski, K. K., Wan, F. Y., Lander, A. D., Calof, A. L., and Nie, Q. (2009) *Math Biosci. Eng.* **6,** 59–82
35. Boukamp, P., Petrussevska, R. T., Breitkreutz, D., Hornung, J., Markham, A., and Fusenig, N. E. (1988) *J. Cell Biol.* **106,** 761–771
36. Schoop, V. M., Mirancea, N., and Fusenig, N. E. (1999) *J. Invest. Dermatol.* **112,** 343–353
37. Ryle, C. M., Breitkreutz, D., Stark, H. J., Leigh, I. M., Steinert, P. M., Roop, D., and Fusenig, N. E. (1989) *Differentiation* **40,** 42–54
38. Jones, P. H., and Watt, F. M. (1993) *Cell* **73,** 713–724
39. Barrandon, Y., and Green, H. (1987) *Proc. Natl. Acad. Sci. U.S.A.* **84,** 2302–2306
40. Boulares, A. H., Yakovlev, A. G., Ivanova, V., Stoica, B. A., Wang, G., Iyer, S., and Smulson, M. (1999) *J. Biol. Chem.* **274,** 22932–22940
41. Hirata, A., Inada, K., Tsukamoto, T., Sakai, H., Mizoshita, T., Yanai, T., Masegi, T., Goto, H., Inagaki, M., and Tatematsu, M. (2004) *J. Histochem. Cytochem* **52,** 1503–1509
42. Jones, P. H., Simons, B. D., and Watt, F. M. (2007) *Cell Stem. Cell* **1,** 371–381
43. Tani, H., Morris, R. J., and Kaur, P. (2000) *Proc. Natl. Acad. Sci. U.S.A.* **97,** 10960–10965
44. Li, A., Simmons, P. J., and Kaur, P. (1998) *Proc. Natl. Acad. Sci. U.S.A.* **95,** 3902–3907
45. Pelengaris, S., Littlewood, T., Khan, M., Elia, G., and Evan, G. (1999) *Mol. Cell.* **3,** 565–577
46. Waikel, R. L., Wang, X. J., and Roop, D. R. (1999) *Oncogene* **18,** 4870–4878
47. Yin, X., Giap, C., Lazo, J. S., and Prochownik, E. V. (2003) *Oncogene* **22,** 6151–6159
48. Frederick, J. P., Liberati, N. T., Waddell, D. S., Shi, Y., and Wang, X. F. (2004) *Mol. Cell. Biol.* **24,** 2546–2559
49. Chen, C. R., Kang, Y., Siegel, P. M., and Massagué, J. (2002) *Cell* **110,** 19–32
50. Yagi, K., Furuhashi, M., Aoki, H., Goto, D., Kuwano, H., Sugamura, K., Miyazono, K., and Kato, M. (2002) *J. Biol. Chem.* **277,** 854–861
51. Maas-Szabowski, N., Stärker, A., and Fusenig, N. E. (2003) *J. Cell Sci.* **116,** 2937–2948
52. Kageyama, R., Ohtsuka, T., Hatakeyama, J., and Ohsawa, R. (2005) *Exp. Cell Res.* **306,** 343–348
53. Dovey, H. F., John, V., Anderson, J. P., Chen, L. Z., de Saint Andrieu, P., Fang, L. Y., Freedman, S. B., Folmer, B., Goldbach, E., Holsztynska, E. J., Hu, K. L., Johnson-Wood, K. L., Kennedy, S. L., Kholodenko, D., Knops, J. E., Latimer, L. H., Lee, M., Liao, Z., Lieberburg, I. M., Motter, R. N., Mutter, L. C., Nietz, J., Quinn, K. P., Sacchi, K. L., Seubert, P. A., Shopp, G. M., Thorsett, E. D., Tung, J. S., Wu, J., Yang, S., Yin, C. T., Schenk, D. B., May, P. C., Altstiel, L. D., Bender, M. H., Boggs, L. N., Britton, T. C., Clemens, J. C., Czilli, D. L., Dieckman-McGinty, D. K., Droste, J. J., Fuson, K. S., Gitter, B. D., Hyslop, P. A., Johnstone, E. M., Li, W. Y., Little, S. P., Mabry, T. E., Miller, F. D., and Audia, J. E. (2001) *J. Neurochem.* **76,** 173–181
54. Kornilova, A. Y., Das, C., and Wolfe, M. S. (2003) *J. Biol. Chem.* **278,** 16470–16473
55. Benitah, S. A., Frye, M., Glogauer, M., and Watt, F. M. (2005) *Science* **309,** 933–935
56. Frye, M., Gardner, C., Li, E. R., Arnold, I., and Watt, F. M. (2003) *Development* **130,** 2793–2808
57. Wilson, A., Murphy, M. J., Oskarsson, T., Kaloulis, K., Bettess, M. D., Oser, G. M., Pasche, A. C., Knabenhans, C., Macdonald, H. R., and Trumpp, A. (2004) *Genes Dev.* **18,** 2747–2763
58. Potten, C. S. (1981) *Int. Rev. Cytol.* **69,** 271–318
59. Jones, P., and Simons, B. D. (2008) *Nat. Rev. Mol. Cell Biol.* **9,** 82–88
60. Clayton, E., Doupé, D. P., Klein, A. M., Winton, D. J., Simons, B. D., and Jones, P. H. (2007) *Nature* **446,** 185–189